Correcting the Effect of LED Spectra on External Quantum Efficiency Measurements of Solar Cells

Appu Paduthol, Mattias K. Juhl, and Thorsten Trupke

***Abstract*—Light emitting diodes (LEDs) are increasingly being used as light sources in studying solar cells due to their high power, low cost, and long bulb lifetimes. However, LEDs do not provide the monochromatic illumination that is desired for an external quantum efficiency measurement. This study investigates the error associated with using a broad emission spectrum instead of monochromatic light on measurements of the external quantum efficiency of silicon solar cells. An analytical approach is used to quantify the impact of the finite spectral width of LEDs. The approach is then extended to provide a method that corrects for the resulting error in the measured external quantum efficiency (EQE). It is shown that after applying the correction method to the measured EQE, the absolute error can be reduced from 1%–2% to under 0.5%.**

***Index Terms*—External quantum efficiency (EQE), light emitting diodes (LEDs).**

I. Introduction

LIGHT emitting diodes (LED) have a practical advantage as a light source as they provide high illumination intensities, with a relatively narrow emission spectrum, and very long bulb lifetimes. It is for this reason that LEDs are now being used in several characterization tools used in photovoltaics [1], [2] including external quantum efficiency (EQE) measurement systems. LED-based systems have shown to be able to extract spatially resolved EQE at a high speed for single and multijunction solar cells [3]–[8]. While a broadband spectrum light source in combination with a monochromator provides light with a narrower spectrum, LEDs can provide higher power and, thus, enable shorter measurement times. This paper first provides a framework to analytically determine the impact of a Gaussian shape illumination spectrum on EQE measurements. A correction procedure is then presented that significantly reduces the error caused by the Gaussian spectrum light source. This approached is then extended to real LED spectra by considering an individual LED spectrum as a composition of several Gaussians. The correction method is experimentally verified for EQE measurements on silicon solar cells using an LED-based EQE measurement system. The method developed is not limited to EQE measurements and can be extended to any wavelength-dependent measurements using a nonmonochromatic light source.

The EQE of a device is the particle collection efficiency, i.e., the number of electrons extracted per incident photon

$$\mathrm{EQE}(\lambda) = \frac{I_{\mathrm{sc}}(\lambda)}{q \cdot N_{\gamma}(\lambda)} \tag{1}$$

where q is the electron charge, $N_{\gamma}(\lambda)$ the incident photon flux, and I_{sc} the extracted current. Equation (1) assumes that the incident illumination is purely monochromatic. However, as an LED has a finite bandwidth, the measured EQE_M is a weighted average

$$\mathrm{EQE}_M(\lambda_0) = \frac{\int_0^{\infty} \mathrm{EQE}(\lambda) \cdot N_{\lambda_0}(\lambda) \cdot d\lambda}{\int_0^{\infty} N_{\lambda_0}(\lambda) \cdot d\lambda} \tag{2}$$

where $N_{\lambda 0}(\lambda)$ is the photon flux per wavelength interval of the LED, and λ_0 is the nominal wavelength. The selection of this nominal wavelength is explained in further sections. The absolute experimental error (U) that results from the finite width illumination source is defined as

$$U(\lambda_0) = \mathrm{EQE}_M(\lambda_0) - \mathrm{EQE}(\lambda_0). \tag{3}$$

II. Theory—Quantification of Error

A mathematical approach was developed to quantify the error in EQE measurements caused by the LED spectra. The approach is first presented for an illumination source with a Gaussian spectral shape, before being extended to real LEDs with non-Gaussian spectra.

An illumination source with a Gaussian shape can be expressed as

$$N_{\lambda}(x) = N_0 \cdot \exp\left(\frac{-(x-\lambda_0)^2}{2 \cdot \sigma^2}\right), \tag{4}$$

where N_0 is the amplitude and σ is the standard deviation. The full width half maxima (FWHM) of the Gaussian spectrum can be defined in terms of σ as $\mathrm{FWHM} = \sigma \times 2\sqrt{2\ln(2)}$. The EQE of a device in (2) is a continuous and differentiable variable, which can be expressed as a Taylor function. This provides for

Manuscript received June 26, 2017; revised October 24, 2017 and December 13, 2017; accepted December 15, 2017. Date of publication January 12, 2018; date of current version February 16, 2018. This work was supported by the Australian Government through the Australian Renewable Energy Agency under Grant RND009. Responsibility for the views, information or advice expressed herein is not accepted by the Australian Government. *(Corresponding author: Appu Paduthol.)*

A. Paduthol and M. K. Juhl are with the University of New South Wales, Sydney NSW 2052, Australia (e-mail: a.paduthol@gmail.com; mattias.juhl@unsw.edu.au).

T. Trupke is with the University of New South Wales, Sydney, NSW 2052, Australia, and also with BT Imaging Pty. Ltd., Sydney, NSW 2017, Australia (e-mail: t.trupke@unsw.edu.au).

Color versions of one or more of the figures in this paper are available online at http://ieeexplore.ieee.org.

Digital Object Identifier 10.1109/JPHOTOV.2017.2787022

the measured $\mathrm{EQE}_M(\lambda_0)$ as

$$\begin{aligned}&\mathrm{EQE}_M(\lambda_0)\\&=\frac{\int_0^\infty \sum_{n=0}^\infty \frac{\mathrm{EQE}^{(n)}(\lambda_0)}{n!}\cdot(x-\lambda_0)^n\cdot\exp\left(-\frac{(x-\lambda_0)^2}{2\cdot\sigma^2}\right)\cdot dx}{\int_0^\infty \exp(-\frac{(x-\lambda_0)^2}{2\cdot\sigma^2})\cdot dx}\\&=\sum_0^\infty \frac{\mathrm{EQE}^{(n)}(\lambda_0)}{n!}\cdot\frac{\int_0^\infty (x-\lambda_0)^n\cdot\exp\left(-\frac{(x-\lambda_0)^2}{2\cdot\sigma^2}\right)\cdot dx}{\int_0^\infty \exp\left(-\frac{(x-\lambda_0)^2}{2\cdot\sigma^2}\right)\cdot dx}\end{aligned} \tag{5}$$

where $\mathrm{EQE}^{(n)}(\lambda_0)$ is the *n*th derivative of EQE curve at λ_0. Equation (5) can be integrated analytically [9] as

$$\begin{aligned}&\mathrm{EQE}_M(\lambda_0)\\&=\sum_{n=0}^\infty \frac{\mathrm{EQE}^{(n)}(\lambda_0)}{n!}\cdot 2^{\frac{n}{2}}\\&\times\frac{\sigma^n\cdot(1+(-1)^n)\cdot\Gamma\left(\frac{1+n}{2},0\right)-(-\sigma)^n\cdot\Gamma\left(\frac{1+n}{2},\frac{\lambda_0{}^2}{2\cdot\sigma^2}\right)}{\sqrt{\Pi}\cdot\left(1+\mathrm{Erf}\left(\frac{\lambda_0}{\sqrt{2}\cdot\sigma}\right)\right)}\end{aligned} \tag{6}$$

where Γ(a, z) is the incomplete Euler function

$$\Gamma(a,x)=\int_x^\infty t^{a-1}\cdot e^{-t}\cdot dt \tag{7}$$

and Erf(x) is the error function given by

$$\mathrm{Erf}(z)=\frac{2}{\sqrt{\Pi}}\cdot\int_0^z e^{-t^2}\cdot dt. \tag{8}$$

In (6), the $n=0$ term is the EQE of the device under test at the wavelength λ_0, i.e., the EQE that is measured by a monochromatic illumination source. Thus, the sum of the remaining terms in (6) represents the error that results from using a Gaussian illumination

$$\begin{aligned}&U(\lambda_0)\\&=\sum_{n=1}^\infty U_n(\lambda_0)=\sum_{n=1}^\infty \frac{\mathrm{EQE}^{(n)}(\lambda_0)}{n!}\cdot 2^{\frac{n}{2}}\\&\times\frac{\sigma^n\cdot(-1)^n\cdot\left(\Gamma\left(\frac{1+n}{2},0\right)-\Gamma\left(\frac{1+n}{2},\frac{\lambda_0{}^2}{2\sigma^2}\right)\right)+\sigma^n\cdot\Gamma\left(\frac{1+n}{2},0\right)}{\sqrt{\Pi}\cdot\left(1+\mathrm{Erf}\left(\frac{\lambda_0}{\sqrt{2}\cdot\sigma}\right)\right)}.\end{aligned} \tag{9}$$

Under the condition that the illumination source's nominal wavelength is much larger than its standard deviation $\lambda_0\gg\sigma$, it is found that $\Gamma(\frac{1+n}{2},0)\gg\Gamma(\frac{1+n}{2},\frac{\lambda_0^2}{2\sigma^2})$ and $\mathrm{Erf}(\frac{\lambda_0}{\sqrt{2}\sigma})\sim 1$. Thus, (9) can be rewritten as

$$\begin{aligned}U(\lambda_0)\approx&\sum_{n=1}^\infty \frac{\mathrm{EQE}^{(n)}(\lambda_0)}{n!}\cdot 2^{\frac{n}{2}}\\&\times\frac{\sigma^n\cdot(1^n+(-1)^n)\cdot\Gamma\left(\frac{1+n}{2},0\right)}{2\cdot\sqrt{\Pi}}.\end{aligned} \tag{10}$$

There are two notable features of (10). First, the term inside the summation is 0 for odd values of *n*. Physically this represents that the impact of an odd function around λ_0 averages to zero, if a symmetric illumination spectrum around λ_0 is used. For e.g., if the EQE changes as a straight line, the measured EQE_M will match the true EQE for Gaussian illumination spectra. This is discussed in more detail in the next section. Second, the terms in the summation decrease quickly with *n* as the sum depends strongly on $2^{\frac{n}{2}}\frac{\Gamma(\frac{1+n}{2})}{n!}$. In this study, we limit *n* to 8, as the impact of further higher values was found to be negligible. To determine the error associated with the even terms, the *n*th derivative $\mathrm{EQE}^{(n)}(\lambda_0)$ is required. This can be determined from experimental data by fitting a high-order polynomial to EQE_M.

III. Error Correction

A simple correction for the error associated with a broad illumination source is found by rearranging of (3)

$$\mathrm{EQE}(\lambda_0)=\mathrm{EQE}_M(\lambda_0)-U(\lambda_0). \tag{11}$$

This correction procedure is now demonstrated with simulations of Gaussian-shaped LED spectra. LEDs were simulated with centre wavelengths ranging from 375 to 1025 nm at every 25 nm and FWHM of 30 nm. The sample investigated was a commercially available silicon photodiode (S2281, Hamamatsu), and is shown in Fig. 1(a). The simulated EQE_M was determined using (2) and is also shown in Fig. 1(a). The derivative of the EQE at each wavelength was determined with a 15 degree polynomial that was fitted to EQE_M. The error term associated with the *n*th derivate of the Taylor series is shown in Fig. 2. There are two notable features here; first, all the odd error terms are 0, in agreement with the above theory. The second is the error falls quickly with the Taylor series order. This was found to be true for all devices tested. Thus, only the first eight terms of *n* in (9) were used for the correction procedure in this paper.

The absolute error between the measured and input data is shown in Fig. 2 before and after correction. The regions with the largest errors are at the short and long wavelengths, where the EQE of the photodiode has some concavity.

The errors for the corrected data shown in Fig. 2 comprise of two components: error from LED's spectral shape and error in the estimated gradient at each wavelength. The error due to the LED's spectral shape can be corrected as discussed above, but this correction depends on the accuracy to which the gradient of the EQE can be determined. It is for this reason the corrected errors are not 0. This is most evident at end points of the data at 375 and 1025 nm. The polynomial fit used to match the EQE is unable to accurately determine the gradient, as the points only have data at either shorter or longer wavelengths.

In the above simulation, a sample set of 27 LEDs were used. Such a high number of evenly spaced data points allows deriving a single polynomial that fits the whole EQE curve. Such a polynomial fit was obtained by applying a least square fit. It was also observed that in cases where a large number of points are not available, a single polynomial fit does not provide a true fit to the actual EQE curve and can lead to false corrections by the model.

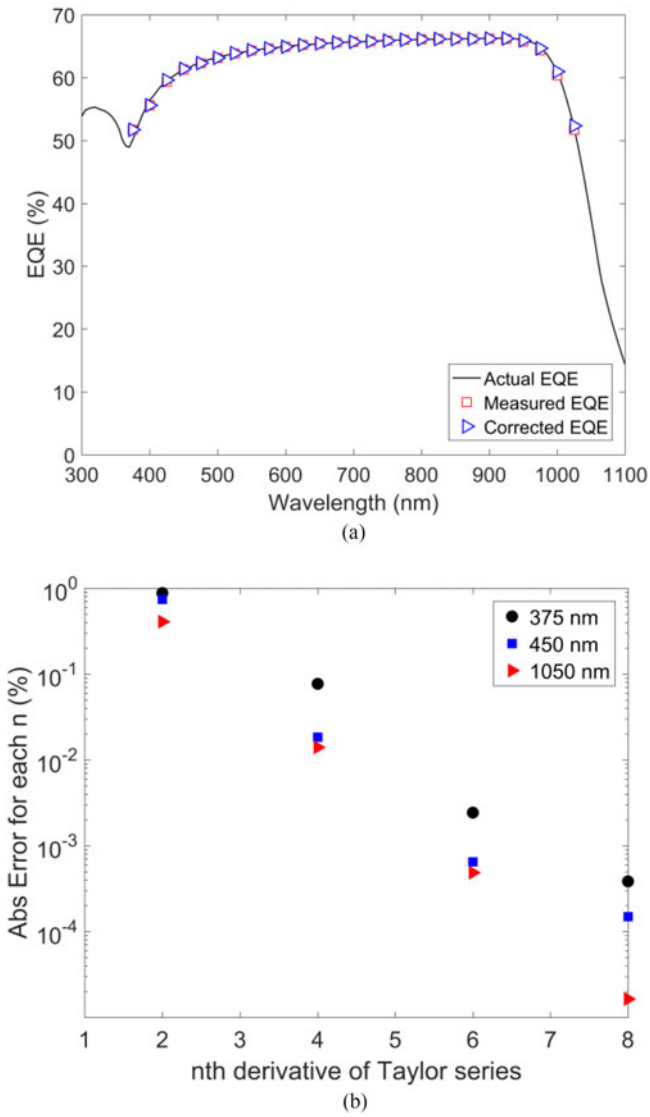

Fig. 1. EQE of a commercial silicon photodiode (line), the as-measured EQE (open squares), and the EQE corrected for the effect of the LED spectra (full triangles), (b) absolute error caused for LEDs with centre wavelengths 375, 450, and 1050 nm, respectively, as a function of n.

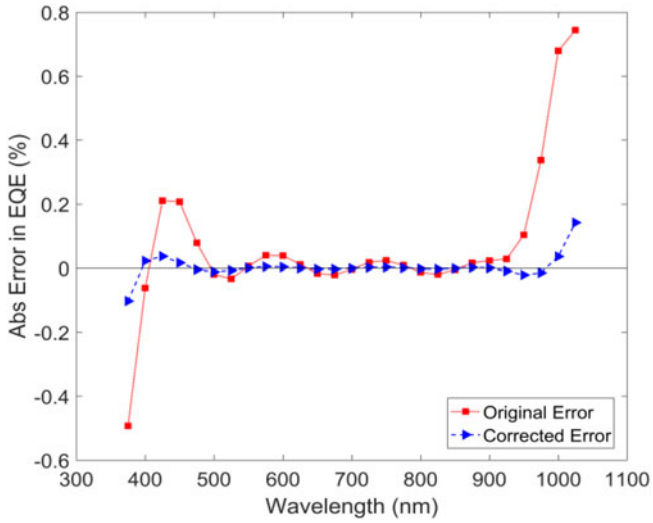

Fig. 2. Error in the measured EQE due to the LED spectra (squares) and the absolute error after correction (triangles) on the EQE curve shown in Fig. 1(a).

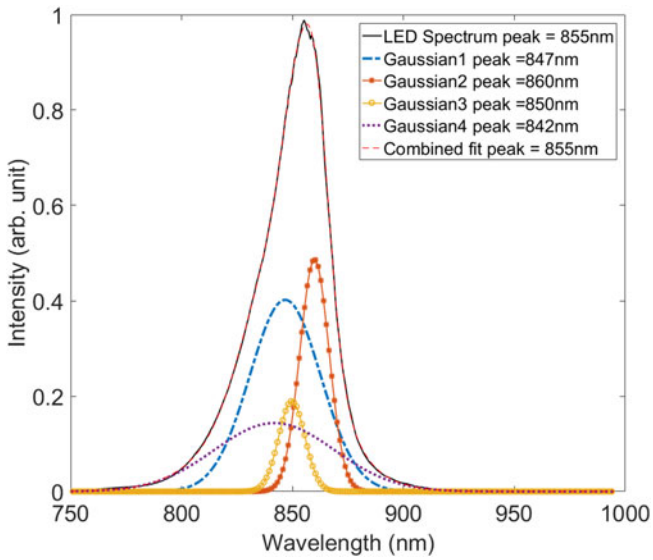

Fig. 3. Spectral emission of LEDs with center wavelength 855 nm, in comparison to a single Gaussian fit and to a weighted sum of four Gaussian curves.

However, in such cases, a piecewise fit can be considered. As shown in Fig. 1(b), the second-order derivate contributes the most to the overall error. Thus, by fitting a second-order polynomial across every three adjacent points, it was seen that an accurate estimate of the gradient can be found. For the experimental verification shown in Section V, such a piecewise fit was performed.

IV. Non-Gaussian Spectrum

In the above sections, it was shown that the error caused by an illumination source with a Gaussian spectral profile can be analytically described. This section extends this method to apply it to real non-Gaussian spectra, enabling applications to real LED spectra. The emission spectrum of a typical LED is generally not accurately described by a single Gaussian curve. However, for the LEDs studied for this paper, the emission of the LED could be modeled as the weighted sum of up to four Gaussians, as shown in Fig. 4. A Gaussian model was used instead of an asymmetric generalized normal distribution because for Gaussian models an analysis similar to that shown in Section II can be used to get the correction terms. More Gaussian terms can be used for light sources with more complex spectra. The illumination spectrum can be defined as

$$N_{\lambda_0}(x) = \sum_{i=1}^{k} W_i \cdot \exp\left(\frac{-(x-\lambda_i)^2}{2 \cdot {\sigma_i}^2}\right) \tag{12}$$

where W_i is the relative weighting, σ_i is the standard deviation, λ_i is the centre wavelength for each Gaussian, and k is the number of Gaussians. As an LED's spectrum is not centred at a single Gaussian, it is assumed that EQE_M is measured at a nominal wavelength λ_0. As an example, the spectrum of an LED with a nominal emission wavelength of $\lambda_0 = 850\,\mathrm{nm}$ is shown in Fig. 3, together with the fitted spectrum and the four

individual Gaussian components. The individual wavelengths and intensities for the four Gaussian components were derived by fitting the terms from (12) to the measured spectrum using trust region method [10]. The coefficients were estimated within 95% confidence bounds. These bounds for the λ_i were found to be within 20 nm for the center peak. The R-square values for these fits were calculated to be above 0.9997.

The error analysis detailed in earlier sections applies for a single Gaussian, i.e., when all $\lambda_i = \lambda_0$. Expanding (2) for an incident illumination spectrum with k weighted Gaussians, the measured EQE will be

$$\mathrm{EQE}_M(\lambda_0) = \frac{\sum_{i=1}^{k} \int_0^{\infty} \mathrm{EQE}(\lambda_i) \cdot N_{\lambda_i}(\lambda) \cdot d\lambda}{\sum_{i=1}^{k} \int_0^{\infty} N_{\lambda_i}(\lambda) \cdot d\lambda} \tag{13}$$

where λ_0 is a nominal wavelength at which the EQE is measured. Similar to the earlier analysis, the expression can be solved as

$$\mathrm{EQE}_M(\lambda_0) = \sum_{n=0}^{\infty} \frac{1}{n!} \cdot 2^{\frac{n}{2}} \times \frac{\sum_{i=1}^{k} W_i \cdot {\sigma_i}^{n+1} \cdot (1 + (-1)^n) \cdot \Gamma(\frac{1+n}{2}, 0) \cdot \mathrm{EQE}^{(n)}(\lambda_i)}{\sum_{i=1}^{k} 2 \cdot \sqrt{\Pi} \cdot (W_i \times \sigma_i)}. \tag{14}$$

At $n = 0$, (14) provides the EQE at the measured wavelength as

$$\mathrm{EQE}(\lambda_0) = \frac{\sum_{i=1}^{k} W_i \cdot \sigma_i \cdot \mathrm{EQE}(\lambda_i)}{\sum_{i=1}^{k} W_i \cdot \sigma_i}. \tag{15}$$

The sum of the remaining terms represents the error term

$$U(\lambda_0) = \sum_{n=1}^{\infty} \frac{1}{n!} \cdot 2^{\frac{n}{2}} \times \frac{\sum_{i=1}^{k} W_i \cdot {\sigma_i}^{n+1} \cdot (1 + (-1)^n) \cdot \Gamma\left(\frac{1+n}{2}, 0\right) \cdot \mathrm{EQE}^{(n)}(\lambda_i)}{\sum_{i=1}^{k} 2 \cdot \sqrt{\Pi} \cdot (W_i \times \sigma_i)}. \tag{16}$$

Now although we have defined the error term and EQE_M, these values are valid at a nominal wavelength, λ_0. The best choice of λ_0 will depend on the spectrum that is being used. If we ensure that all the values of λ_i are close to the centre wavelength, then the EQE in that small wavelength interval can be assumed to be linear. Under this assumption, (15) allows the definition of λ_0 as

$$\lambda_0 = \frac{\sum_{i=1}^{k} W_i \cdot \sigma_i \cdot \lambda_i}{\sum_{i=1}^{k} W_i \cdot \sigma_i}. \tag{17}$$

This definition of λ_0 allows us to specify the nominal wavelength at which the EQE is measured by each LED, independent of the measured sample. This λ_0 can be interpreted as the centre of mass of the LED's spectrum as it is an average of the centre wavelength weighted by the amplitude and FWHM of the Gaussian.

In summary, the error correction defined by (16) at λ_0 can be used with (11) to get a corrected EQE. In the next section, we demonstrate this correction method experimentally.

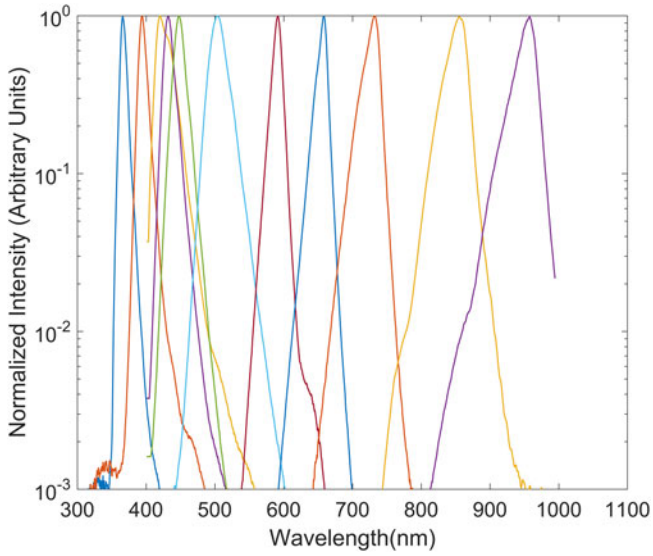

Fig. 4. Spectral emission of the 11 LEDs used for experimental verification. The intensity of the LEDs ranged from 50 to 150 W/m^2.

V. Experimental Verification

The correction procedure outlined above was applied to an LED-based large signal [11] EQE system constructed at University of New South Wales. This system comprised of an LED light source (future LED GmbH) that consists of 11 LEDs. The spectra of the LEDs were measured with a spectrometer (IsoPlane 160, Princeton Instruments ProEM 1600) and are shown in Fig. 4. The absolute photon flux of each LED was determined using a calibrated silicon photodiode. The intensity of the LEDs was monitored *in situ* with a reference photodiode. The device under test was connected to a low noise current amplifier (Femto DLPCA 200). The output voltage of the reference photodiode and the photodiode under test was monitored with a 16-bit data acquisition card (Measurement Computing USB1608).

The EQE of a germanium photodiode and of a silicon photodiode were measured. The samples' true EQE was determined with a commercial diffusive monochromator-based system (QEX10, PV Measurements) with a spectral resolution of 5 nm. The statistical error in the EQE_M data was determined from 10 repeat measurements to be less than 0.03% absolute.

The EQE determined by the commercial EQE system is shown in Figs. 5(a) and 6(a) as solid lines. The EQE for these photodiodes were measured with the LED and the correction procedure was then applied. Here a second-order polynomial was fitted to every three adjacent points of EQE_M to determine the Taylor series. The error caused by the LED spectrum was corrected via (15), (16). The initial EQE_M and the corrected EQE_C are shown in Figs. 5(a) and 6(a). The as-measured deviation between the measured data and the error after correcting for the LED spectra is shown in Figs. 5(b) and 6(b) as red dashed lines and blue dashed lines, respectively.

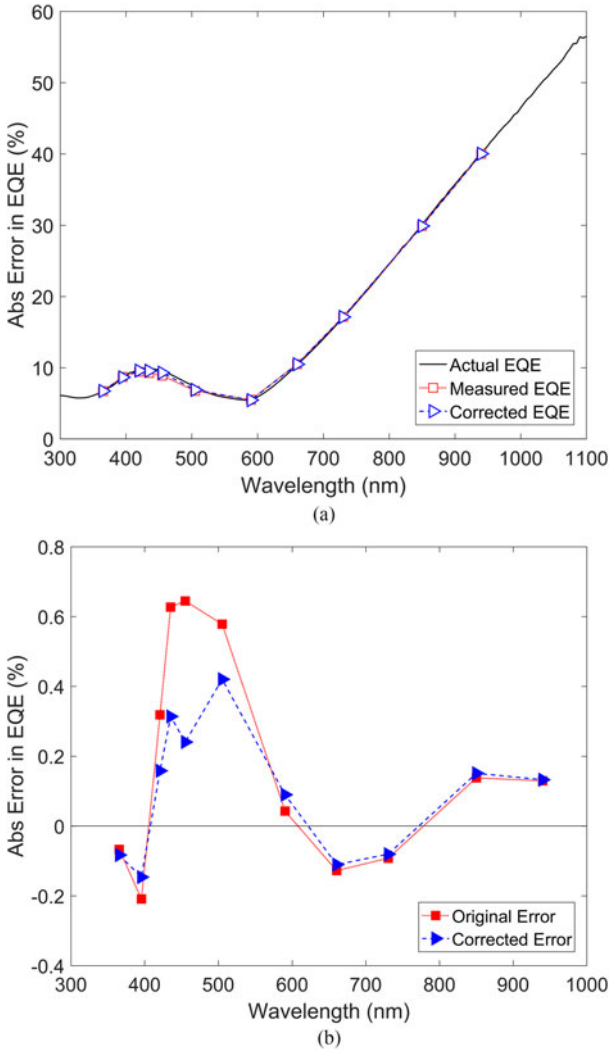

Fig. 5. (a) EQE of the Ge photodiode, (b) error in the LED-based measurement before and after the correction procedure.

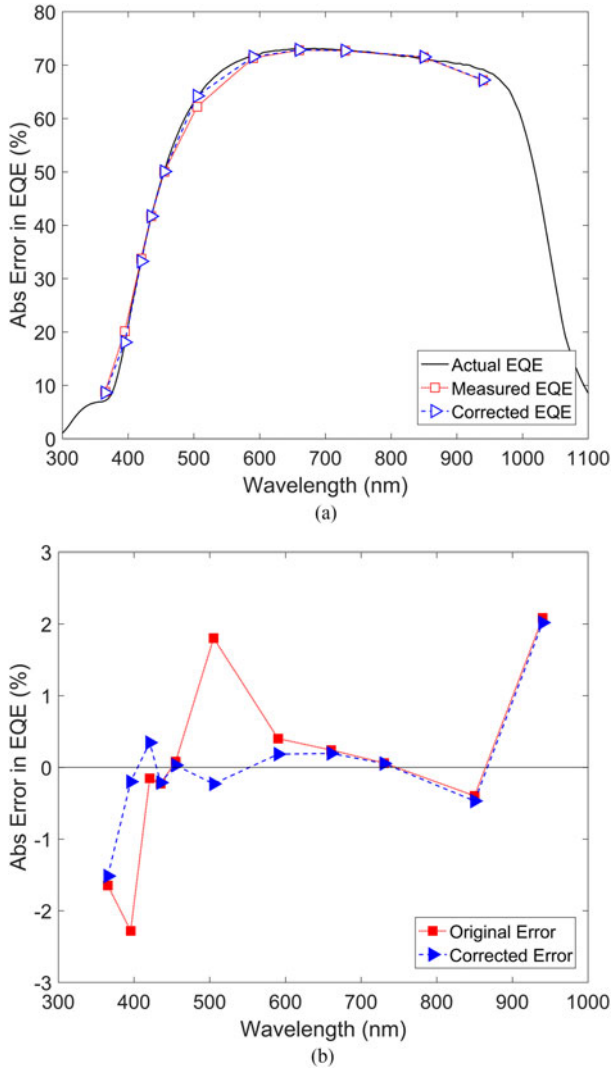

Fig. 6. Demonstration of the correction procedure on a silicon photodiode. (a) EQE determined for a Si photodiode; (b) error in the LED-based measurement before and after the correction procedure.

The EQE of the Ge photodiode in the 600–1000 nm range is linear and, therefore, has very small second-order derivatives. The measurements show the errors in the linear region of the EQE to be small, however, the error is not zero. The remaining uncertainty is expected to arise from differences between the systems, and is taken as a limit to which the two systems can be compared.

The same procedure was repeated for the Silicon photodiode (see Fig. 6). The method clearly reduces the errors for wavelength with high second derivatives in EQE. For points with already low error, the no real change is seen. These points have a similar error as the Ge photodiode, and are expected to arise from a different source. This method fails to correct the first and the last points in the EQE curve (365 and 950 nm). As mentioned above, this occurs as the derivative of the EQE at these points is not accurately described by the polynomial. The impact of these outside points can be reduced by using a closer spacing of LEDs Thus, if the first and last points are ignored, the errors arising from the LEDs spectra are reduced from greater than 2% to below 0.5%.

Other than the spectral shape of the LED, an error in calibrating the light source, capacitance of the device being measured, or electrical noise during measurement can also result in an error in the measured EQE. The total error in the measurement of EQE is limited by the largest error source in the system. The approach shown here assumes that the spectral shape of the LED is the dominant source of error. As shown in the results in Figs. 5(b) and 6(b), it can be concluded that the correction procedure is limited by the noise floor of the errors from other sources.

VI. Conclusion

The experimental uncertainty in measuring EQE on solar cells with LED illumination with finite spectral width was studied. An analytical description of the errors that result from using a light source with a Gaussian spectral shape was determined. It was shown that the errors arising from the spectral shape of the LEDs depend on the shape of the LED's spectra and the second-order derivative of the EQE curve at the excitation

wavelength. This analytical description was then used to correct experimental EQE data from an LED-based system.

It was shown that errors arising from the spectral width of the LEDs can be reduced. The final error is comparable to the uncertainty that we measured in a conventional monochromator-based EQE system. The method was tested using a system comprising of 11 LEDs with centre wavelengths ranging from 365 to 950 nm on silicon and germanium samples. The errors arising from the LED's spectra were shown to be reduced by the technique. It must be noted that the method relies on representing the EQE curve of a device as a piecewise polynomial curve. Thus, the accuracy of the method depends significantly on the number of LEDs. We emphasize that the analysis presented here is not limited to EQE measurements but is relevant and can be applied to any measurement of wavelength-dependent parameters, for example transmission and reflection measurements.

REFERENCES

[1] F. C. Krebs, K. O. Sylvester-Hvid, and M. Jørgensen, "A self-calibrating led-based solar test platform," *Progress Photovolt. Res. Appl.*, vol. 19, no. 1, pp. 97–112, Jan. 2011.

[2] D. L. Young, B. Egaas, S. Pinegar, and P. Stradins, "A new real-time quantum efficiency measurement system," in *Proc. 33rd IEEE Photovolt. Spec. Conf.*, 2008, pp. 1–3.

[3] T. Luka, S. Eiternick, and M. Turek, "Rapid testing of external quantum efficiency using LED solar simulators," *Energy Procedia*, vol. 77, pp. 113–118, 2015.

[4] G. S. Horner *et al.*, "Flash quantum efficiency measurements for multi-junction solar cells," in *Proc. 37th IEEE Photovolt. Spec. Conf.*, 2011, pp. 1716–1720.

[5] T. Missbach, C. Karcher, and G. Siefer, "Frequency-division-multiplex-based quantum efficiency determination of solar cells," *IEEE J. Photovolt.*, vol. 6, no. 1, pp. 266–271, Jan. 2016.

[6] J. A. Rodríguez, M. Fortes, C. Alberte, M. Vetter, and J. Andreu, "Development of a very fast spectral response measurement system for analysis of hydrogenated amorphous silicon solar cells and modules," *Mater. Sci. Eng., B*, vol. 178, no. 1, pp. 94–98, Jan. 2013.

[7] J. Schmidt *et al.*, "Characterization and gauge study of a high speed quantum efficiency apparatus," in *Proc. 35th IEEE Photovolt. Spec. Conf.*, 2010, pp. 1710–1714.

[8] W. Reetz *et al.*, "A novel high speed spectral response measurement system based on LED light sources," in *Proc. 26th Eur. Photovolt. Sol. Energy Conf. Exhib.*, Jan. 2011, pp. 113–116.

[9] E. W. Weisstein, "Gaussian integral," *MathWorld–A Wolfram*, Oct. 2017. [Online]. Available: http//mathworld.wolfram.com/GaussianIntegral.html

[10] J. J. Moré and D. C. Sorensen, "Computing a trust region step," *SIAM J. Sci. Statist. Comput.*, vol. 4, no. 3, pp. 553–572, Sep. 1983.

[11] H. Mäckel and A. Cuevas, "Capturing the spectral response of solar cells with a quasi-steady-state, large-signal technique," *Progress Photovolt. Res. Appl.*, vol. 14, no. 3, pp. 203–212, May 2006.

Authors' photographs and biographies not available at the time of publication.